WDR19 Expression is Increased in Prostate Cancer Compared with Normal Cells, but Low-Intensity Expression in Cancers is Associated with Shorter Time to Biochemical Failures and Local Recurrence

Biaoyang Lin,[1,2,3] Angelita G. Utleg,[2] Karsten Gravdal,[5] James T. White,[2] Ole J. Halvorsen,[5] Wei Lu,[2] Lawrence D. True,[3] Robert Vessella,[3] Paul H. Lange,[3] Peter S. Nelson,[4] Leroy Hood,[2] Karl-Henning Kalland,[5] and Lars A. Akslen[5]

Abstract

Purpose: Prostate cancer is the third leading cause of cancer death in the United States, following lung and colorectal cancer. We previously identified *WDR19* as a prostate-specific, androgen-regulated gene. Here, we evaluate its utility as a prostate cancer tissue marker for diagnosis and prognostic evaluation.

Experimental Design: Real-time quantitative PCR was done on a panel of prostate tissue isolated by laser capture microdissection. After generating antibodies against WDR19, tissue microarrays (TMA) were employed to compare WDR19 expression between normal, benign prostatic hyperplasia, and prostate cancer tissue.

Results: Using microarrays and real-time quantitative PCR, we showed that *WDR19* mRNA expression was increased in cancer. We further showed that WDR19 protein is localized to cytoplasmic subcellular granules and is expressed exclusively in prostate epithelia. Large-scale immunohistochemical staining using TMAs reveals a significant percentage of increase in intensely staining tissue cores in cancer tissue when compared with normal or benign prostatic hyperplastic tissue. Based on the analysis of a separate TMA for which clinical follow-up information was available, low-intensity WDR19 staining was significantly associated with decreased time to biochemical failure ($P = 0.006$) and with decreased time to locoregional recurrence ($P = 0.050$).

Conclusions: WDR19 should be added to the list of prostate cancer tissue markers. The continued expansion of a multiple-marker panel will conceivably increase the sensitivity and specificity of prostate cancer diagnosis and prognosis.

Prostate cancer is the third leading cause of cancer death, following lung and colorectal cancer, in the United States. The American Cancer Society estimated 218,890 new cases and ~27,050 deaths in the United States in 2007 (1). Early diagnosis is important because low-stage cancer is more effectively treated by surgery or radiation compared with high-stage tumors. However, early diagnosis can generate lead-time bias, and consequently, improved 5-year survival of patients with prostate cancer (2). After diagnosis, the key question is how the patient will respond to treatment and how long the patient will survive. However, our capacity to predict the prognosis of patients with prostate cancer is limited.

Better markers are therefore needed to both diagnose and predict disease course more accurately. Recent progress has led to the identification of many candidate markers for prostate cancer, including *NKX3.1*, *KLK2*, *KLK3 (PSA)*, *FOLH1 (PSMA)*, *STEAP2*, *PSGR*, *PRAC*, *RDH11*, Prostein, Hepsin, α-methylacyl CoA racemase (*AMACR*), *FASN*, *EZH2* (3), and Huntingtin-interacting protein 1 (4). Effective markers need not only be tumor antigens, but could also be autoantibodies, such as those for Huntingtin-interacting protein 1 and those for 22 peptides

identified by phage display (5, 6). Despite this progress, there is still no individual marker that can segregate tumors with a clinically benign behavior. It is generally believed that a multiple biomarker panel is important to increase the sensitivity and specificity in early diagnosis, and to increase the accuracy in predicting disease outcome and monitoring treatment efficacy.

We report here the identification of WDR19 as another tissue marker for prostate cancer. We show, using microarrays and real-time quantitative PCR (qPCR), that WDR19 mRNA expression increases in prostate cancer. Generating antibodies against WDR19 permitted us to determine that WDR19 protein is expressed solely in prostate epithelia and is localized to subcellular granules. Large-scale immunohistochemical staining using tissue microarrays (TMA) revealed a significantly increased percentage of tissue cores with intense WDR19 staining in cancer compared with normal or benign prostatic hyperplasia (BPH) tissue. Finally, we found that low-intensity WDR19 staining is significantly associated with decreased time to biochemical failure ($P = 0.006$) and with decreased time to locoregional recurrence ($P = 0.050$) within the group of prostate cancers. This protein may be added to the list of prostate cancer tissue markers, thereby helping expand the multiple-marker panel needed to increase diagnostic and prognostic sensitivity and specificity.

Materials and Methods

cDNA microarray analysis. A custom-built cDNA microarray (PEDB Array; refs. 7, 8) was used. This array contains 6,000 cDNAs printed in four replicates on the same slide. The cDNA was labeled with Cy5 as we described previously (8, 9). Spotfinding was done using AnalyzerDG software (MolecularWare, Inc.).

Real-time qPCR. The RNA and cDNA preparation from prostate cancer tissues and cells were previously described (10). TaqMan Gene Expression Assay kits for *WDR19* and *HPRT* were obtained from Applied Biosystems, Inc. The PCR reactions were done using the ABI Prism 7900HT Sequence Detection System and SDS Enterprise Database (Applied Biosystems Inc.). PCR variables were 50°C for 2 min, 95°C for 10 min, then 40 cycles with each cycle at 95°C for 15 s and 60°C for 1 min. Relative quantification for real-time qPCR was done using the mathematical model and formula published by Pfaffl (11).

WDR19 protein expression and purification. A region of 126 amino acids corresponding to amino acids 824 to 949 was cloned in-frame with the glutathione *S*-transferase (GST) fusion expression vector pGEX-4T-1 (GE Healthcare Bio-Sciences, Corp.). In detail, oligonucleotide primers (GTGGATCCATGGGAGACATACGTCGAGGG and TTGAATTCTCACTGGGTCTCTCTAACAATATT) were designed to amplify cDNA corresponding to amino acids 824 to 949 of the WD repeat coding region. The cDNA template was prepared from 40 µg of total RNA that was obtained from LNCaP cells grown in the presence of 1 nmol/L of synthetic androgen R1881 as described (12). The following PCR profile was used: (*a*) 94°C for 4 min; (*b*) 94°C for 30 s, 55°C for 30 s, 72°C for 1 min, 35 cycles; (*c*) 72°C at 7 min final extension; and (*d*) 4°C overnight. The expected 394-bp PCR product amplified by Stratagene pfu polymerase (Stratagene Inc.) was cloned into the expression vector, pGEX-4T-1 (GE Healthcare Bio-Sciences Corp.). The accuracy and orientation of the construct was confirmed by sequencing and restriction enzyme digestion and analysis.

Escherichia coli BL21 cells [strain: F-, ompT, hsdS (r_B^-, m_E^-)] were used for GST fusion protein expression. One BL21 colony with the expression construct was picked and grown in 2XYTA medium, induced with a final concentration of 0.4 mmol/L of isopropyl-L-thio-β-D-galactopyranoside during the exponential growth stage, and grown at 30°C for 6 h. The fusion protein was prepared using a freeze-thaw method (GE Healthcare Bio-Sciences, Corp.) and purified using a HiTrap affinity column purchased from GE Healthcare Bio-Sciences Corp., and the EP-1 Econo Pump from Bio-Rad, Inc.

WDR19 monoclonal antibody production. The production of hybridoma was subcontracted to the Biologics Production Department, headed by Dr. Elizabeth Wayner, at the Fred Hutchinson Cancer Research Center. A standard mouse hybridoma production method was used. Differential screening by ELISA against WDR19-GST fusion protein and GST protein alone was conducted to identify hybridomas that bound only to the WDR19 proteins. Positive hybridomas were confirmed by Western blot analysis using LNCaP cell lysates. Monoclonal hybridomas were obtained through limited dilution followed by selection of single colonies using a light microscope. The supernatant from the monoclonal hybridomas were then tested against WDR19 proteins using ELISAs and Western blots. The monoclonal hybridoma cells were grown in RPMI 1640 with 10% fetal bovine serum, 2 mmol/L of L-glutamine, 1% sodium pyruvate, gentamicin, and an adenine/aminopterin/thymidine medium (Sigma-Aldrich). Supernatants from hybridoma cultures were collected after 95% of the cells had died (~ 12 to 14 days). The supernatant was filtered through a 0.2-µm filter and tested against a LNCaP lysate blot before purification. The antibody was then purified by gravity flow using first a column of Sepharose 4B and then a column of protein L (Sigma-Aldrich) each with a 2 mL bed volume. The columns were washed with 30 mL of 1× PBS, and the protein was eluted in 0.1 mol/L of a glycine solution at pH 2.0. Fractions with protein were dialyzed in 1× PBS overnight at 4°C followed by protein concentration determination with the Bradford assay.

Competition assay. Eight microliters of WDR19 mouse monoclonal antibody 9E1N1 (2.3 µg total) were mixed with 10 or 25 µg of 9E1N1-GST fusion protein into the tube, and the volume was brought to 200 µL of 1× PBS. As a control, 8 µL of 9E1N1 antibody (2.3 µg total) was added to 192 µL of 1× PBS in another tube. The tubes were rocked at 4°C overnight. The immunocomplexes were then pelleted at 14,000 rpm for 30 min. One hundred and eighty microliters of the supernatant was collected from each tube and added to 4 mL of blocking solution (5% milk/2% normal goat serum/0.1% Tween 20). The secondary antibody titer used for LNCaP blots was 1:5,000 anti–IgG₁-HRP (Southern Biotech) and 1:10,000 anti–IgG₁-HRP (0.4 mg/mL) for the sera blots. The blots were incubated at room temperature for 1 h and then washed thrice with 1× PBS-0.1% Tween 20, each time for 20 min at room temperature. The enhanced chemiluminescence reagents from GE Biosciences were used for band detection.

Immunohistochemical analysis. Paraffin-embedded prostate cancer tissue sections obtained from the laboratory of Robert Vessella at the University of Washington were used to optimize immunohistochemical conditions. TMA arrays with 34 prostate cancer tissue cores (one specimen per patient) were prepared at the Pacific Northwest Prostate Cancer Specialized Programs of Research Excellence core by Dr. Larry True (Dept. of Pathology, University of Washington, Seattle, WA; ref. 13). Multiple tissue array slides were also obtained from the National Cancer Institute Cooperative Prostate Cancer Tissue Resource[6] for comparing normal, BPH, and prostate cancer tissues. The National Cancer Institute TMA contained 278 prostate cancer tissue cores, 15 BPH cores, and 13 normal tissue cores (all with one specimen per patient). All sections to be immunostained were deparaffinized, hydrated, boiled with 10 mmol/L of citrate buffer (pH 6) for 10 min, treated with 0.3% H_2O_2 for 5 min, preincubated in blocking solution (5% normal sera from horse, cow, and goat in 1× PBS buffer) for 1 h at

---

[6] http://www.cpctr.info.gov

Fig. 1. *A,* schematic plot of microarray data for 10 prostate cancer tissues (*T*) and 11 normal adjacent tissues (*N*). *X*-axis, normalized intensity values. Bars, SD. *B,* box and whiskers plot of real-time qPCR data for WDR19 expression in normal adjacent prostate cells, prostate cancer cells (*CaP*), and prostate cancer metastasis (*Cap_mets*). *Y*-axis, relative expression levels. *C,* pair-wise comparison of *WDR19* transcript expression in normal adjacent prostate cells and prostate cancer cells. Normalized real-time qPCR data were plotted. *X*-axis, sample pairs; *Y*-axis, relative expression levels.
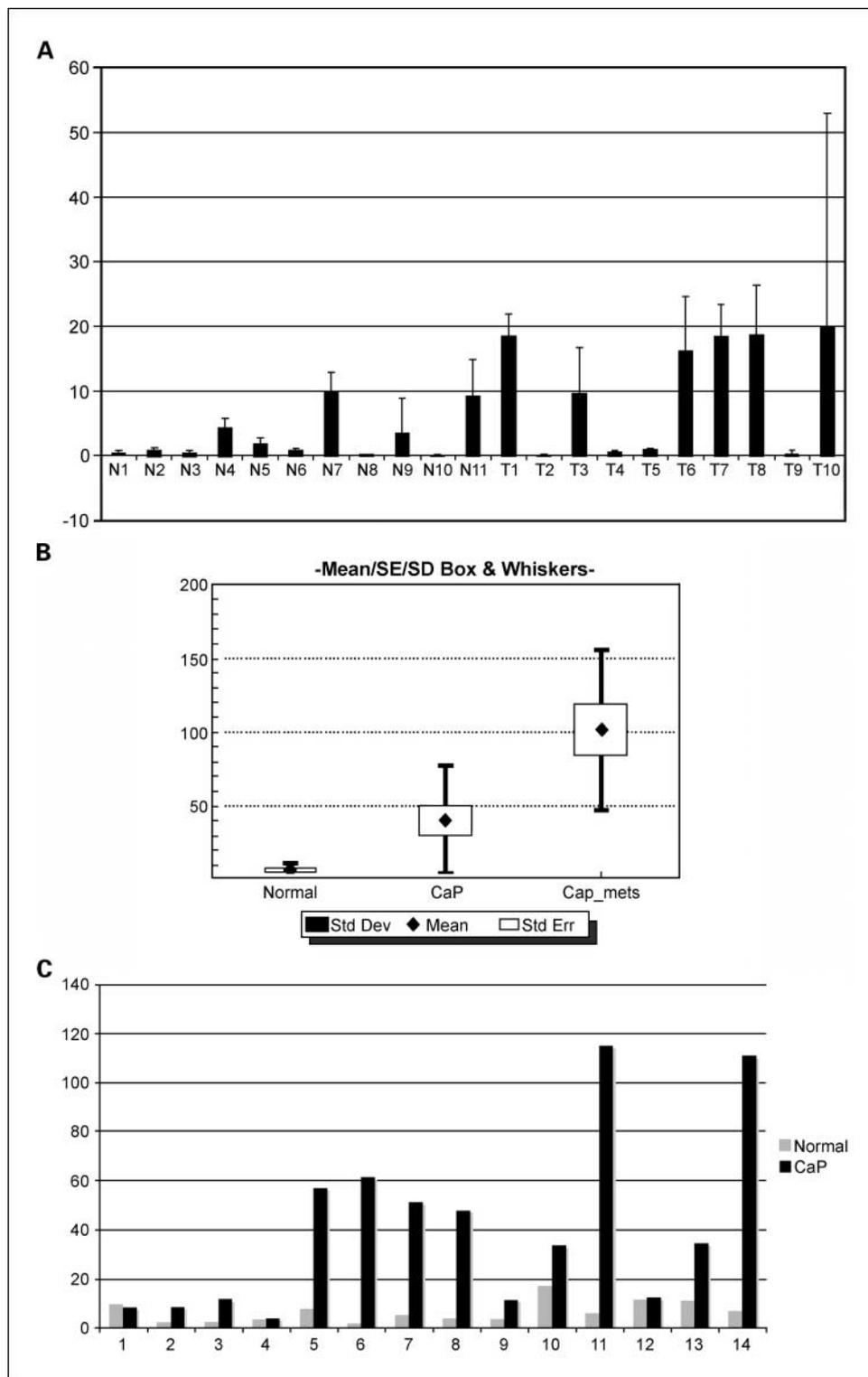
room temperature, and incubated with the primary antibody (purified WDR19 antibody 9E1N1, diluted 1:50) for 16 to 18 h at 4°C. The sections were then washed with PBS and processed with an avidin-biotin complex immunoperoxidase staining system. The avidin-biotin complex method involves three sequential steps: (*a*) primary antibody, (*b*) biotin-labeled secondary antibody, and (*c*) avidin-biotin peroxidase complex. Immunostaining was visualized by treating the sections with 0.05% 3,3-diaminobenzidine and 0.01% hydrogen peroxide in PBS.

Culture media/PBS was used as a negative control. The avidin-biotin complex reagents were purchased from Vector Laboratories. The optimal dilution used for the biotinylated secondary antibody (mouse IgG) was 1:200 diluted in blocking solution. The immunohistochemical staining intensity of WDR19 was based on the staining intensity of a majority of cells and was scored as negative (1), faint/equivocal (2), moderate (3), or strong (4), similar to the criteria used by Rubin et al. (14). To test for differences in the staining intensity among different cell

types, we used a multiple regression model and an ANOVA for the regression. Immunohistochemical scores were imported into the GB STAT program (Dynamic Microsystems, Inc.) for the analysis.

We also examined a separate TMA established at The Gade Institute, University of Bergen, including tissue cores represented in triplicate (0.6 mm diameter) from 104 prostatic adenocarcinomas obtained from radical prostatectomy specimens and clinicopathologic information. Immunostains were carried out as described (15). We used a staining index (SI; values 0-9) with the following formula: SI = intensity × positive area, where intensities were scored as 0 (negative), 1 (faint/equivocal), 2 (moderate), and 3 (strong). Immunoreactive areas were categorized as 0 (0%), 1 (<10%), 2 (10-50%), 3 (>50%).

Statistical analysis. For microarray data analysis, mean spot intensity minus local background intensity for each spot was imported into the GeneSpring Program 7.3 (Agilent, Inc.), and normalization schema was to normalize to the 50th percentile per chip and normalize to the median per gene. Background-subtracted intensities of four replicate spots were averaged. An intensity (after background subtraction) cutoff value of 400 (approximately twice the SD of the background values) was used as a threshold to remove weak hybridization signals. A nonparametric test (Wilcoxon-Mann-Whitney test) with a P value of 0.05 and a multiple testing correction (Benjamini and Hochberg false discovery rate) of 0.05 was applied and the resulting list of genes was considered differentially expressed.

Time from surgery to biochemical failure (defined as persistent or rising serum prostate-specific antigen (PSA) levels of >0.5 ng/mL in two consecutive blood samples) was noted. Furthermore, a tumor in the prostatic fossa or evidence of distant metastasis on bone scan, X-ray, or MRI was recorded as clinical recurrence. As described previously (16, 17), a consecutive series of 104 men treated by radical prostatectomy for clinically localized prostate cancer during 1988 to 1994, with long and complete follow-up, was included in this study. Clinical stage T_1/T_2 disease, negative bone scan, and generally good health, were the prerequisites for radical retropubic prostatectomy. The majority of cancers in this series are clinical stage T_2 and presented

before the PSA era started in Norway in the mid-1990s. Consequently, the prevalence of adverse prognostic factors such as capsular penetration, seminal vesicle invasion, and positive surgical margins is rather high compared with most contemporary series. No patients treated by radical prostatectomy received radiotherapy prior to biochemical failure or clinical recurrence.

Statistical analysis of WDR19 staining and its correlations with clinicopathologic variables were done using the SPSS program (SPSS, Inc.). Pearson's χ^2 test was applied to compare WDR19 staining index and clinicopathologic variables. Multivariate survival analyses were done according to Cox's proportional hazards regression model to evaluate the predictive values of WDR19 staining index and clinicopathologic variables.

Results

WDR19 mRNA levels are elevated in prostate cancer tissues compared with benign adjacent tissues. We have systematically characterized androgen-responsive genes in prostate cancer cells (2), and isolated and characterized a new androgen-regulated gene, designated *WDR19* by the Human Gene Nomenclature Committee because it encodes WD-repeating sequence motifs common to the WD repeat family of proteins. The tissue distribution of *WDR19* transcripts was assessed by Northern blotting and dot-blot assays using RNAs derived from multiple human tissues. *WDR19* was found to be most highly expressed in the human prostate from a dot-blot assay comparing 76 human tissues (12).

Using a custom-built cDNA microarray—the PEDB array (7), we hybridized cDNAs from 10 prostate cancer tissues and 11 normal adjacent prostate tissues. The array was printed in four replicates on the same slide and the cDNA was labeled with Cy5 as we described previously (8). Statistical analysis using
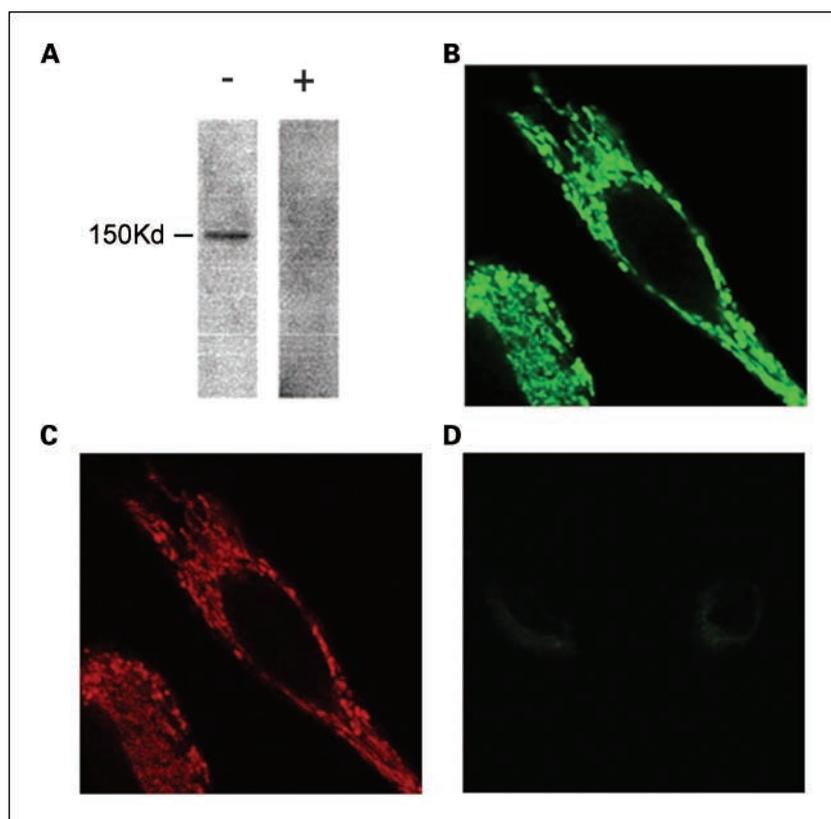
Fig. 2. *A,* competition assay for the WDR19 antibody 9E1N1. Lane -, no preincubation with purified WDR19 protein; lane +, preincubation with purified WDR19 protein. Lysates from prostate cancer cell line LNCaP cells were used for the Western blot analysis. *B,* LNCaP cells were stained with mouse sera against WDR19 protein. The secondary antibody is goat anti-mouse IgG conjugated to fluorescein Texas red. *C,* the same cells were stained with rabbit anti-prostate acid phosphatase antibody. The secondary antibody is goat anti-rabbit IgG conjugated to FITC. *D,* LNCaP cells stained only with goat anti-mouse IgG conjugated with FITC dye.

Wilcoxon-Mann-Whitney test ($P = 0.05$) and a multiple testing correction (Benjamini and Hochberg false discovery rate) of 0.05 revealed that 542 genes (147 down-regulated and 395 up-regulated genes comparing tumor tissues with normal tissues based on average expression values) are significantly differentially expressed (Supplementary Table S1).

Included in this list were both known genes involved in prostate carcinogenesis, including *KLK2, KLK3, KLK4, NKX3.1, TMEPA1, TMPRSS2, PSMA, AMACR, ERBB3*, four CD markers (*CD9, CD44, CD59,* and *CD164*), and many novel proteins not previously characterized (Supplementary Table S1). Many interesting genes not previously shown to be involved in prostate cancer appeared, including three genes with WD repeat domains: *WDR19, FBXW5* (F-box and WD40 domain protein 5), and *WDR68*. Another interesting protein identified is ELF3, an epithelial specific ETS domain transcription factor, in light of the recent identification of recurrent fusion of TMPRSS2 and ETS transcription factor genes in prostate cancer (18).

Because we were most interested in prostate-specific genes overexpressed in prostate cancer, and we previously showed that *WDR19* is a prostate-enriched/specific gene (12), we picked WDR19 for further follow-up analysis. The expression of *WDR19* in 10 prostate cancer tissues and 11 normal adjacent prostate tissues is shown in Fig. 1*A*. The Wilcoxon-Mann-Whitney test *P* values were 0.0099 (Supplementary Table S1). We then did a real-time qPCR for *WDR19* on a panel of 15 prostate cancer specimens, and 15 matched-paired specimens from adjacent normal prostate tissues. We also included 10 metastatic prostate cancer specimens from 10 different patients. Each specimen consisted of ~5,000 cells isolated by laser capture microdissection. PCR products from all samples showed a single band by gel electrophoresis (data not shown). The real-time qPCR data were quantified using the mathematical model published by Pfaffl (11), and then the data were subjected to statistical analysis. The HPRT gene was used as an endogenous control as it was identified by de Kok et al. as the best control for normal and cancer tissue comparisons among 13 frequently used housekeeping genes that they tested (19). A sample from the cancer group (sample C7) failed to PCR and was removed from the analysis. Analysis with the Student's *t* test showed that the mRNA expression levels of *WDR19* were significantly different between normal prostate epithelial cells and localized prostate cancer, between normal prostate epithelial cells and metastasized prostate cancer, and between localized and metastasized prostate cancers, with *P* values of 0.00064, 0.00158, and 2.8E-07, respectively (one-tail distribution, homoscedastic). Analyses using other tail and variance options also resulted in significant *P* values. All data were graphed with the box-and-whisker plot (Fig. 1*B*), and the expression levels of *WDR19* in 14 matched pairs of normal prostate and prostate cancer biopsies are shown in Fig. 1*C*.

We were not able to perform an analysis to evaluate the significance of using *WDR19* as a prognostic marker using these reverse transcription-PCR data because the sample sizes were too small.

WDR19 protein is expressed only in prostate epithelial cells and is localized to subcellular granules. To evaluate whether WDR19 is more highly expressed at the protein level in prostate cancer tissue, we developed a mouse monoclonal antibody against WDR19. A DNA fragment corresponding to amino acids 824 to 949 of WDR19 was cloned into pGEX4.1 to
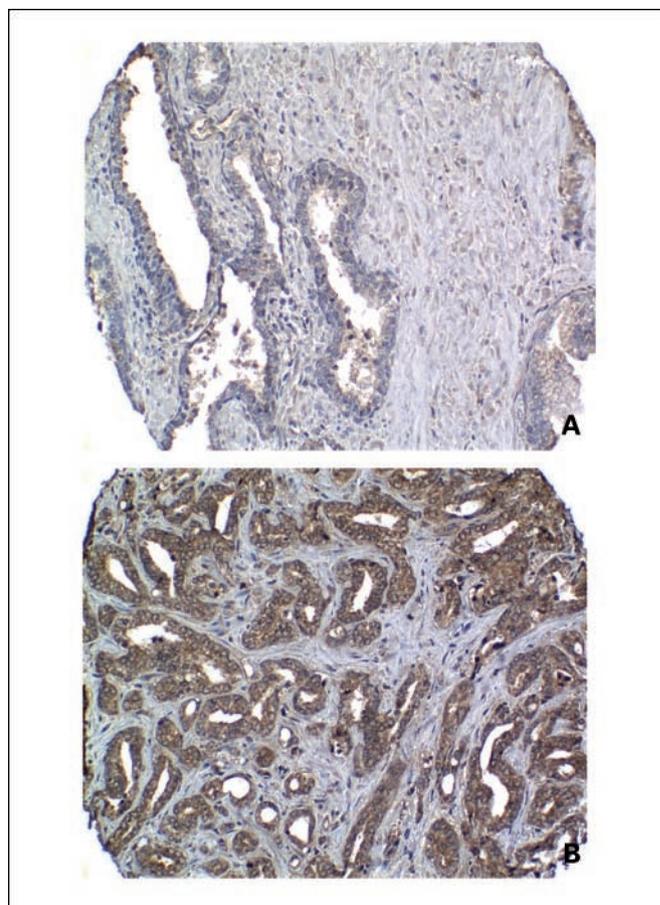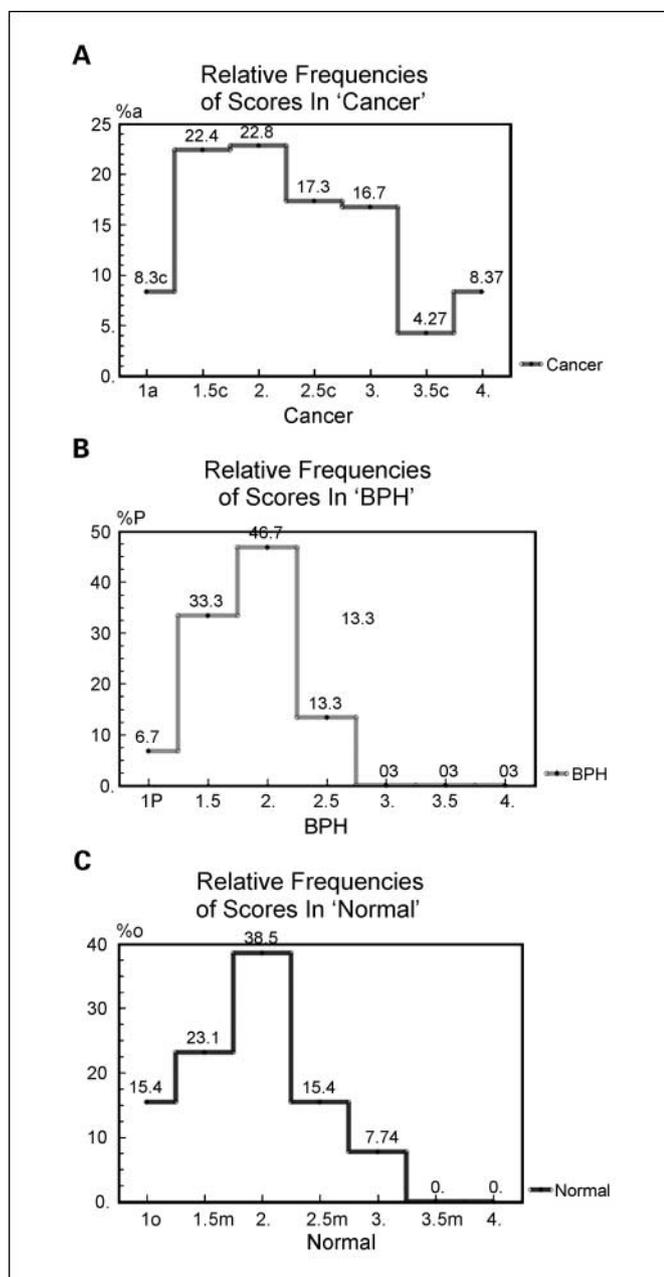

Fig. 3. Immunohistochemical staining of prostate tissue sections. Examples of cores from a TMA stained with WDR19 antibody 9E1N1. Top, normal prostate gland showing little or very weak staining of epithelia; bottom, cancer glands showing strong cytoplasmic staining.

express a GST fusion protein (GST-WDR19). The GST fusion protein was expressed in *E. coli*, purified, and used to immunize mice using standard protocols (20). Differential ELISA screening using GST-WDR19 and purified GST was done to select positive hybridoma clones and rule out antibodies specific for the GST moiety. Limited dilution of positive hybridomas was done, and subsequent clones were screened by ELISA, Western blot, and immunohistochemistry of cultured LNCaP cells. The specificities of antibodies for endogenous WDR19 were established by a competitive ELISA, employing the combination of preincubation with GST-WDR19 recombinant protein with antibody titration (Fig. 2*A*). These results indicated that our monoclonal antibody was specific to WDR19 in LNCaP lysate.

We did cell staining to identify the subcellular location of WDR19 in LNCaP cells. Our data indicated that WDR19 was expressed in subcellular granules in LNCaP cells (Fig. 2*B-D*) as it colocalized with prostatic acid phosphatase, which is expressed primarily in the lysosomal granules of LNCaP cells (21).

WDR19 protein expression is elevated in cancer tissues. Tissue sections from both cancer and adjacent benign tissue showed that the WDR19 antibody stained luminal epithelial cells, whereas no significant staining was observed in the tumor stroma. The staining also showed that WDR19 is more highly expressed in cancer compared with benign tissue (Fig. 3).

Fig. 4. Step plot of relative frequencies (percentages) of average immunohistochemical staining scores in normal, BPH, and prostate cancer TMA cores. *X*-axis, immunohistochemistry scores with 0.5 step increments; *Y*-axis, frequencies at each step of the immunohistochemical staining scores.

In order to determine whether our initial observation of elevated WDR19 expression in prostate cancer applies to a larger sample population, we obtained high-density TMAs of prostate tissue consisting of >300 cores from the National Cancer Institute's Cooperative Prostate Cancer Tissue Resource.[5] We also obtained a TMA of prostate tissues from the specimen core at the Pacific Northwest Prostate Cancer Specialized Programs of Research Excellence program. We quantified the expression level (staining intensity) of epithelial cells in localized prostate cancer, BPH, and normal prostate gland in the high-density TMA; 278 prostate cancer tissue cores, 15 BPH cores, and 13 normal tissue cores had corresponding cores on both TMA

slides (some of the cores were empty on one slide, or contained no epithelial cells). Both TMAs were stained and scored by an experienced pathologist. Additionally, 34 prostate cancer specimens were obtained from the Pacific Northwest Prostate Cancer Specialized Programs of Research Excellence, stained and scored on replicated TMA arrays. WDR19 expression was scored as negative (1), faint/equivocal (2), moderate (3), or strong (4), similar to the criteria used by Rubin et al. (14) for their TMA analysis. The scores from the two TMAs were averaged for comparison. For prostate cancer tissues, 91 of the 312 (29.2%) tissue cores had an average score of >3. In contrast, only 1 of the 13 normal (7.7%) and none of the 15 BPH cores had an average score of >3. The distribution of score frequencies in normal, BPH, and cancer is shown in Fig. 4. ANOVA for multiple regression analysis revealed *P* values of 0.0075 and 0.0007 for normal versus cancer tissues and BPH versus cancer tissues, respectively. WDR19 staining showed no significant difference between the BPH and normal prostate tissue.

Low-intensity expression of WDR19 in prostate cancer is associated with shorter time to biochemical failure and local recurrence. To investigate whether the expression of WDR19 is

Table 1. Cytoplasmic staining of WDR19 in tumor cells and associations with clinicopathologic characteristics (*n* = 104); Pearson's χ^2 analysis

Variable	No.	WDR19		P
		(0-3)	(6-9)	
Tumor diameter*				ns
<31 mm	78	23	55	
>31 mm	25	11	14	
Gleason score †				0.012
≤3 + 4	49	10	39	
≥4 + 3	55	24	31	
Capsular penetration ‡				ns
Absent	32	7	25	
Present	72	27	45	
Seminal vesicle invasion				ns
Absent	69	21	48	
Present	35	13	22	
Clinical stage				0.061
T_{1b}, N_0, M_0	9	6	3	
T_{1c}, N_0, M_0	3	0	3	
T_{2a}, N_0, M_0	58	17	41	
T_{2b}, N_0, M_0	25	10	15	
$T2_c, N_0, M_0$	9	1	8	
Pathologic stage§				0.079
pT_2	30	6	24	
$≥pT_3$	74	28	46	
Lymph nodes‖				ns
Absent	97	31	66	
Present	7	3	4	
Ki-67¶				0.051
<Median	51	12	39	
>Median	53	22	31	

Abbreviation: ns, not significant.
*Largest tumor dimension in prostatectomy specimen.
† Standard Gleason score in radical prostatectomy specimens.
‡ Capsular penetration.
§Pathologic stage, tumor-node-metastasis.
‖Pelvic lymph node infiltration at radical prostatectomy.
¶Proliferation in tumor cells estimated by Ki-67.

correlated with any clinical behavior of prostate cancers, we additionally analyzed TMAs from 104 prostate samples (in triplicate, 312 cores) from 104 different individuals from The Gade Institute in Norway. Because all the clinicopathologic information was available for these samples (Table 1), we were able to determine whether the WDR19 staining index was associated with any clinicopathologic variables. After analysis, the distributions by the WDR19 staining index (SI) were: SI = 3, 34 cases; SI = 6, 65 cases; SI = 9, 5 cases. To simplify the data, we categorized the WD repeat staining pattern into faint staining (SI = 0-3; 34 cases in total) and intense staining (SI = 6-9; 70 cases in total). Using a statistical analysis (Pearson's χ^2 test), we found that faint WDR19 staining was marginally associated with more advanced clinical stage ($P = 0.061$), and more advanced pathologic stage ($P = 0.079$; Table 1). Furthermore, we found that faint WDR19 staining was significantly associated with total Gleason score $\geq 4 + 3$ ($P = 0.012$; Table 1; Fig. 5) and poor (high) histologic grade, as defined by the WHO ($P = 0.001$; data not shown). Using univariate survival analysis, we also found that faint WDR19 staining was significantly associated with shorter time to biochemical failure ($P = 0.006$) and locoregional recurrence ($P = 0.050$; Table 1; Fig. 5).

We then did multivariate survival analyses for time to biochemical failure, time to clinical recurrence, and for time to locoregional metastases (Table 2). We also compared WDR19 expression to basic variables, such as preoperative s-PSA, total Gleason score ($\leq 3 + 4$ versus $\geq 4 + 3$) and pathologic stage (pT). For biochemical failure, only total Gleason score [hazard ratios (HR), 3.3; $P < 0.0005$], pT (HR, 2.5; $P = 0.006$), and preoperative s-PSA (HR, 1.6; $P = 0.089$) showed an independent prognostic effect. For time to locoregional metastases, only total Gleason score (HR, 4.1; $P = 0.003$) showed an independent prognostic effect. For time to clinical recurrences, only total Gleason score (HR, 5.0; $P < 0.0005$) showed an independent prognostic effect (Table 2). Thus, we found that low-level WDR19 expression in early prostate cancer was significantly associated with more aggressive tumor subgroups. This was, however, without independent prognostic effect in multivariate survival analysis.

Discussion

We have shown herein that a novel marker, WDR19, is overexpressed in prostate cancers at the transcriptional level

Fig. 5. Survival analysis (Kaplan-Meier method) of patients with prostate cancer ($n = 104$) using different end points. Low-intensity WDR19 staining was significantly associated with shorter time to biochemical failure ($P = 0.006$; A) and also associated with shorter time to locoregional recurrences ($P = 0.05$; C).
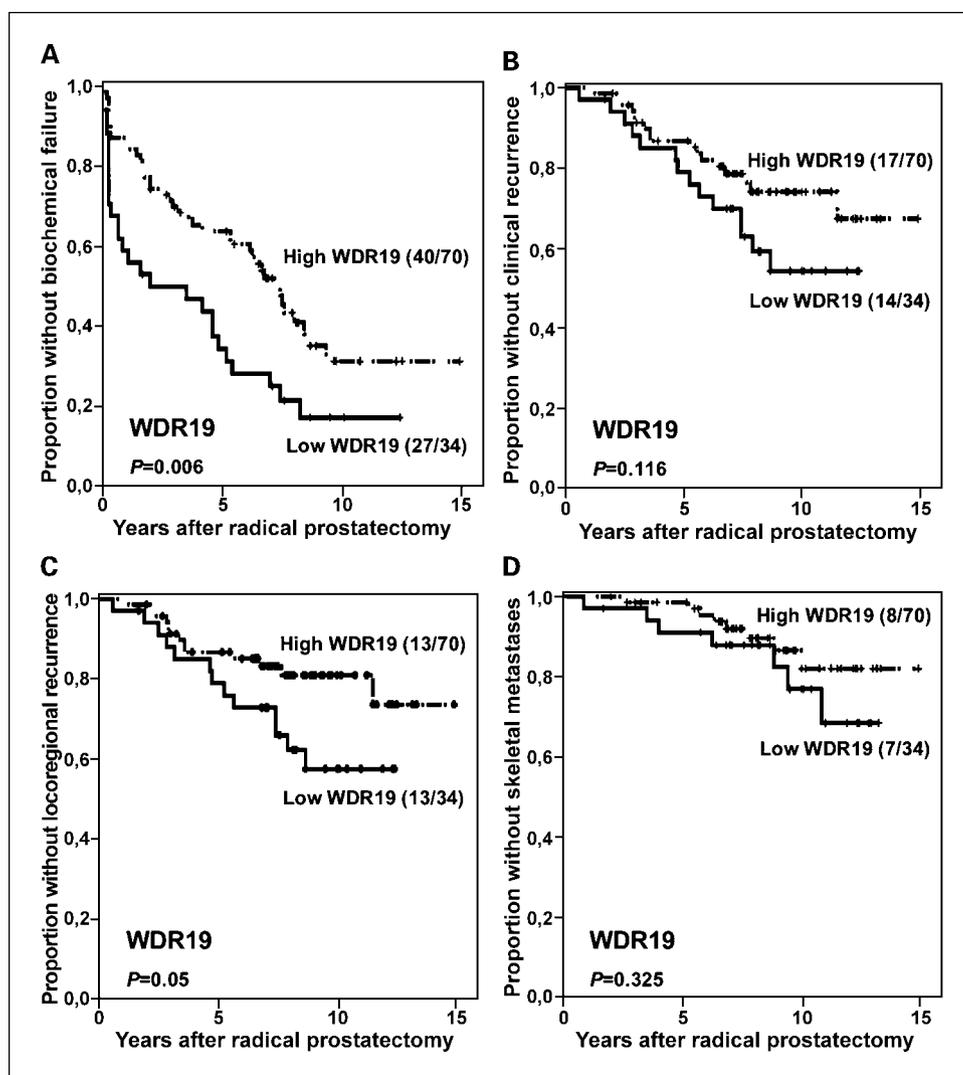
using real-time qPCR and DNA microarrays. Using immunohistochemistry staining on prostate TMAs, we have further shown that WDR19 is expressed in epithelial cells, and that high WDR19 protein expression was observed more frequently in cancer tissues compared with normal or BPH samples. Therefore, WDR19 seems to be a novel prostate cancer marker.

We observed that faint WDR19 staining (i.e., low expression) was significantly associated with high-grade tumors (increased Gleason score and WHO histologic grade) and shorter time to biochemical failure ($P = 0.006$) and locoregional tumor recurrence ($P = 0.050$; Table 1; Fig. 5). Because WDR19 is an androgen-regulated gene (12) and is related to a more differentiated state, it is not surprising to find lower WDR19 protein expression levels in the androgen-independent tumors, which are often present in patients with high Gleason scores. That does not, however, explain the observed contradiction that *WDR19* mRNA is overexpressed in prostate cancer that metastasize to distant organs (Fig. 1*B*). It is possible that mRNA level and protein levels do not always correlate. In fact, global comparisons of proteomics and transcriptomics data provide many such examples (22, 23). Furthermore, the metastatic cells in Fig. 1*B* were taken from distant organs (not from the prostate), so their change in microenvironment might subject them to altered regulation by a variety of growth factors and hormones (24–26). In addition, it is likely that the local level of androgens in distant organs may differ from that in the prostate.

WDR19 expression is higher in prostate cancer compared with BPH, but a lower expression in localized cancer is associated with worse clinical outcomes compared with a higher expression. We searched for genes with similar expression patterns in prostate cancer. We found that AMACR was overexpressed in prostate cancer relative to benign prostatic tissue (14) and is highly expressed in prostate cancer metastases (27). Recently, Rubin et al. showed that lower AMACR tissue expression in localized prostate cancer, determined by immunohistochemistry, was associated with less favorable outcome (HR, 3.7 for PSA failure; $P = 0.018$; HR, 4.1 for prostate cancer death, $P = 0.0006$). They showed that among patients with both low AMACR expression and high Gleason score, the risk of prostate cancer death increased 18-fold ($P = 0.006$; ref. 28). KAI1/CD82 was overexpressed in prostate cancers compared with BPH (29, 30). Its expression is increased in well and moderately differentiated cancers compared with BPH, but is decreased in poorly differentiated cancers showing aggressive cancer behavior (29, 31). Hepsin is overexpressed in prostate cancer but its expression in primary prostate cancer correlates inversely with measures of patient prognosis (32). Multivariate analysis of TMA staining of hepsin indicated an association of weak or absent hepsin protein expression with increased risk of PSA elevation following prostatectomy and a high Gleason score [corresponding HRs were 2.9 ($P = 0.0004$) and 1.65 ($P = 0.037$), respectively; ref. 32]. ALCAM/CD166 was overexpressed in low-grade prostate cancer but its expression is progressively lost in high-grade lesions (33).

A multiple-marker panel is crucial for obtaining a highly sensitive and specific cancer diagnosis tool. Various prostate

Table 2. Multivariate survival analysis according to Cox's proportional hazards method for patients with localized prostate cancer using biochemical failure, clinical recurrence, and locoregional metastases as end points

Variable	Category	n	HR (95% confidence interval)	P*
Biochemical failure				
Gleason score	≤3 + 4	43	1.0	0.000
	≥4 + 3	55	3.3 (1.8-5.8)	
Pathologic stage	≤pT$_2$	30	1.0	0.006
	≥pT$_3$	68	2.5 (1.2-4.9)	
Preoperative s-PSA	Low	73	1.0	0.089
	High	25	1.6 (0.9-2.9)	
WDR19	High	66	1.0	0.114
	Low	32	1.5 (0.9-2.7)	
Clinical recurrence				
Gleason score	≤3 + 4	43	1.0	<0.0005
	≥4 + 3	55	5.0 (1.7-14.5)	
Pathologic stage	≤pT$_2$	30	1.0	0.119
	≥pT$_3$	68	2.2 (0.7-6.3)	
Preoperative s-PSA	Low	73	1.0	0.96
	High	25	1.0 (0.5-2.3)	
WDR19	High	66	1.0	0.92
	Low	32	1.0 (0.5-2.2)	
Locoregional metastases				
Gleason score	≤3 + 4	43	1.0	0.003
	≥4 + 3	55	4.1 (1.4-12)	
Pathologic stage	≤pT$_2$	30	1.0	0.247
	≥pT$_3$	68	1.8 (0.6-5.4)	
Preoperative s-PSA	Low	73	1.0	0.665
	High	25	1.2 (0.5-2.9)	
WDR19	High	66	1.0	0.341
	Low	32	1.5 (0.7-3.4)	

*Likelihood ratio test.

cancer studies have identified a wide variety of both proteins and autoantibodies as potential biomarkers. The clinical utility of multiple markers is already becoming apparent. Recently, Rhodes et al. tried to use a multiplex biomarker approach for determining the risk of PSA-defined recurrence of prostate cancer. They screened 14 candidate biomarkers for prostate cancer, including hepsin, pim-1 kinase, E-cadherin (ECAD; cell adhesion molecule), AMACR, and EZH2 (enhancer of zeste homologue 2, a transcriptional repressor) and showed that statistically significant ratios of EZH2/ECAD were associated with prostate cancer recurrence. This remained true even after adjusting for clinical variables, such as tumor stage, Gleason score, and PSA level (HR, 3.19; 95% confidence interval, 1.50 to 6.77; $P = 0.003$; ref. 34). We believe WDR19 will have cancer diagnostic utility, and based on our observed differential expression between different cancer types, WDR19 could also be valuable as a prognostic tool. However, we want to emphasize that the survival of patients with metastatic prostate cancers was not studied here. The outcomes of the range of protein immunohistochemical staining applies only to localized cancers. We have not analyzed a large set of metastasized prostate cancer samples by immunohistochemical staining. Although we have analyzed 10 metastasized prostate cancer samples by reverse transcription-PCR, the sample size was too small for a prognostic analysis.

The function of WDR19 in prostate development and function, and in prostate carcinogenesis, remains to be investigated. WD repeat proteins are a large family of proteins that are implicated in a variety of functions ranging from signal transduction and transcription regulation to cell cycle control and apoptosis. Putative orthologues of WDR19 in *Caenorhabditis elegans* and *Drosophila* were recently identified (35, 36). They all contained WD40 repeat units, tetratricopeptide repeats, and clathrin heavy chain repeat. WD40 repeats and tetratricopeptide repeats play important roles in protein-protein interactions

------

[7] http://www.ebi.ac.uk/interpro/

and clathrin heavy chain repeat plays important roles in endocytosis.[7] DYF-2, the *C. elegans* orthologue of WDR19, is involved in intraciliary/intraflagellar transport. Loss of DYF-2 function selectively affects the assembly and motility of different intraflagellar transport components and leads to defects in cilia structure and chemosensation in *C. elegans* (35). The mouse WDR19 was shown to localize to granule structures inside of the cell at the base of cilia in the ependymal cells lining the ventricles of the mouse brain (35). Interestingly, recent studies revealed that multiple components of the Sonic hedgehog and platelet-derived growth factor receptor-α signal transduction pathways localize to the primary cilium, and that loss of the cilium blocks ligand-induced signaling by both pathways (37). It was reported that the Sonic hedgehog pathway was involved in tumor progression and metastases of prostate cancer (38). However, because prostate cancer cells lack cilia, the relationship between the granular structures to which WDR19 is localized, and the role of these structures in prostate carcinogenesis remains to be investigated.

In summary, WDR19 expression seems to follow a complex pattern during prostate cancer progression. We observed that its expression was increased from normal adjacent tissues to localized cancer tissues (using real-time qPCR of laser capture–microdissected cells). In localized cancer tissues, its expression was inversely correlated with Gleason score and high (poor) histologic grade (using immunohistochemical staining). Finally, its expression was again increased in the metastasized cancers compared with localized cancers (using real-time qPCR of laser capture–microdissected cells). This suggests that WDR19 expression is regulated by a complex mechanism involving androgen receptor signaling and other yet unidentified signaling pathways.

Acknowledgments

References

1. Jemal A, Siegel R, Ward E, et al. Cancer statistics, 2007. CA Cancer J Clin 2007;57:43–66.

2. Chinnaiyan A, Coffey D, Forrest S, et al. Merging bottom-up and top-down approaches to study prostate cancer biology. Complexity 2002;7:22–30.

3. Tricoli JV, Schoenfeldt M, Conley BA. Detection of prostate cancer and predicting progression: current and future diagnostic markers. Clin Cancer Res 2004; 10:3943–53.

4. Rao DS, Hyun TS, Kumar PD, et al. Huntingtin-interacting protein 1 is overexpressed in prostate and colon cancer and is critical for cellular survival. J Clin Invest 2002;110:351–60.

5. Wang X, Yu J, Sreekumar A, et al. Autoantibody signatures in prostate cancer. N Engl J Med 2005;353: 1224–35.

6. Bradley SV, Oravecz-Wilson KI, Bougeard G, et al. Serum antibodies to huntingtin interacting protein-1: a new blood test for prostate cancer. Cancer Res 2005;65:4126–33.

7. Nelson PS, Pritchard C, Abbott D, Clegg N. The human (PEDB) and mouse (mPEDB) prostate expression databases. Nucleic Acids Res 2002;30: 218–20.

8. Lin B, Ferguson C, White JT, et al. Prostate-localized and androgen-regulated expression of the membrane-bound serine protease TMPRSS2. Cancer Res 1999; 59:4180–4.

9. Nelson PS, Clegg N, Arnold H, et al. The program of androgen-responsive genes in neoplastic prostate epithelium. Proc Natl Acad Sci U S A 2002;99:11890–5.

10. Lu W, Zhou D, Glusman G, et al. KLK31P is a novel androgen regulated and transcribed pseudogene of kallikreins that is expressed at lower levels in prostate cancer cells than in normal prostate cells. Prostate 2006;66:936–44.

11. Pfaffl MW. A new mathematical model for relative quantification in real-time RT-PCR. Nucleic Acids Res 2001;29:e45.

12. Lin B, White JT, Utleg AG, et al. Isolation and characterization of human and mouse WDR19, a novel WD-repeat protein exhibiting androgen-regulated expression in prostate epithelium. Genomics 2003; 82:331–42.

13. True L, Coleman I, Hawley S, et al. A molecular correlate to the Gleason grading system for prostate adenocarcinoma. Proc Natl Acad Sci U S A 2006; 103:10991–6.

14. Rubin MA, Zhou M, Dhanasekaran SM, et al. α-Methylacyl coenzyme A racemase as a tissue biomarker for prostate cancer. JAMA 2002;287: 1662–70.

15. Halvorsen OJ, Rostad K, Oyan AM, et al. Increased expression of SIM2-s protein is a novel marker of aggressive prostate cancer. Clin Cancer Res 2007;13: 892–7.

16. Gravdal K, Halvorsen OJ, Haukaas SA, Akslen LA. Expression of bFGF/FGFR-1 and vascular proliferation related to clinicopathologic features and tumor progress in localized prostate cancer. Virchows Arch 2006;448:68–74.

17. Halvorsen OJ, Haukaas S, Hoisaeter PA, Akslen LA. Independent prognostic importance of microvessel density in clinically localized prostate cancer. Anticancer Res 2000;20:3791–9.

18. Tomlins SA, Rhodes DR, Perner S, et al. Recurrent fusion of TMPRSS2 and ETS transcription factor genes in prostate cancer. Science 2005;310:644–8.

19. de Kok JB, Roelofs RW, Giesendorf BA, et al. Normalization of gene expression measurements in tumor tissues: comparison of 13 endogenous control genes. Lab Invest 2005;85:154–9.

20. Azorsa DO, Moog S, Cazenave JP, Lanza F. A general approach to the generation of monoclonal antibodies against members of the tetraspanin superfamily using recombinant GST fusion proteins. J Immunol Methods 1999;229:35–48.

21. Warhol MJ, Longtine JA. The ultrastructural localization of prostatic specific antigen and prostatic acid phosphatase in hyperplastic and neoplastic human prostates. J Urol 1985;134:607–13.

22. Lin B, White JT, Lu W, et al. Evidence for the presence of disease-perturbed networks in prostate cancer cells by genomic and proteomic analyses: a

systems approach to disease. Cancer Res 2005;65:
3081 – 91.

23. Chen G, Gharib TG, Huang CC, et al. Discordant
protein and mRNA expression in lung adenocarcino-
mas. Mol Cell Proteomics 2002;1:304 – 13.

24. Culig Z, Bartsch G. Androgen axis in prostate can-
cer. J Cell Biochem 2006;99:373 – 81.

25. Gennigens C, Menetrier-Caux C, Droz JP. Insulin-
like growth factor (IGF) family and prostate cancer.
Crit Rev Oncol Hematol 2006;58:124 – 45.

26. Zhu B, Kyprianou N. Transforming growth factor β
and prostate cancer. Cancer Treat Res 2005;126:
157 – 73.

27. Luo J, Zha S, Gage WR, et al. α-Methylacyl-CoA
racemase: a new molecular marker for prostate
cancer. Cancer Res 2002;62:2220 – 6.

28. Rubin MA, Bismar TA, Andren O, et al. Decreased
α-methylacyl CoA racemase expression in localized
prostate cancer is associated with an increased rate

of biochemical recurrence and cancer-specific
death. Cancer Epidemiol Biomarkers Prev 2005;14:
1424 – 32.

29. Lijovic M, Somers G, Frauman AG. KAI1/CD82 pro-
tein expression in primary prostate cancer and in BPH
associated with cancer. Cancer Detect Prev 2002;26:
69 – 77.

30. Bouras T, Frauman AG. Expression of the prostate
cancer metastasis suppressor gene KAI1 in primary
prostate cancers: a biphasic relationship with tumour
grade. J Pathol 1999;188:382 – 8.

31. Ueda T, Ichikawa T, Tamaru J, et al. Expression of the
KAI1 protein in benign prostatic hyperplasia and
prostate cancer. Am J Pathol 1996;149:1435 – 40.

32. Dhanasekaran SM, Barrette TR, Ghosh D, et al.
Delineation of prognostic biomarkers in prostate
cancer. Nature 2001;412:822 – 6.

33. Kristiansen G, Pilarsky C, Wissmann C, et al.
ALCAM/CD166 is up-regulated in low-grade prostate

cancer and progressively lost in high-grade lesions.
Prostate 2003;54:34 – 43.

34. Rhodes DR, Sanda MG, Otte AP, Chinnaiyan AM,
Rubin MA. Multiplex biomarker approach for determin-
ing risk of prostate-specific antigen-defined recurrence
of prostate cancer. J Natl Cancer Inst 2003;95:661 – 8.

35. Efimenko E, Blacque OE, Ou G, et al. *Caenorhabdi-
tis elegans* DYF-2, an orthologue of human WDR19, is
a component of the intraflagellar transport machinery
in sensory cilia. Mol Biol Cell 2006;17:4801 – 11.

36. Avidor-Reiss T, Maer AM, Koundakjian E, et al.
Decoding cilia function: defining specialized genes
required for compartmentalized cilia biogenesis. Cell
2004;117:527 – 39.

37. Michaud EJ, Yoder BK. The primary cilium in cell
signaling and cancer. Cancer Res 2006;66:6463 – 7.

38. Sheng T, Li C, Zhang X, et al. Activation of the
hedgehog pathway in advanced prostate cancer. Mol
Cancer 2004;3:29.

Clinical Cancer Research

WDR19 Expression is Increased in Prostate Cancer Compared with Normal Cells, but Low-Intensity Expression in Cancers is Associated with Shorter Time to Biochemical Failures and Local Recurrence

Biaoyang Lin, Angelita G. Utleg, Karsten Gravdal, et al.

Clin Cancer Res 2008;14:1397-1406.

Updated version	Access the most recent version of this article at: http://clincancerres.aacrjournals.org/content/14/5/1397
Supplementary Material	Access the most recent supplemental material at: http://clincancerres.aacrjournals.org/content/suppl/2008/03/03/14.5.1397.DC1

Cited articles	This article cites 38 articles, 13 of which you can access for free at: http://clincancerres.aacrjournals.org/content/14/5/1397.full#ref-list-1
Citing articles	This article has been cited by 1 HighWire-hosted articles. Access the articles at: http://clincancerres.aacrjournals.org/content/14/5/1397.full#related-urls

E-mail alerts	Sign up to receive free email-alerts related to this article or journal.
Reprints and Subscriptions	To order reprints of this article or to subscribe to the journal, contact the AACR Publications Department at pubs@aacr.org.
Permissions	To request permission to re-use all or part of this article, use this link http://clincancerres.aacrjournals.org/content/14/5/1397. Click on "Request Permissions" which will take you to the Copyright Clearance Center's (CCC) Rightslink site.